

# VD3D: Taming Large Video Diffusion Transformers for 3D Camera Control

Sherwin Bahmani<sup>1,2,3</sup> Ivan Skorokhodov<sup>3</sup> Aliaksandr Siarohin<sup>3</sup> Willi Menapace<sup>3</sup>  
 Guocheng Qian<sup>3</sup> Michael Vasilkovsky<sup>3</sup> Hsin-Ying Lee<sup>3</sup> Chaoyang Wang<sup>3</sup>  
 Jiaxu Zou<sup>3</sup> Andrea Tagliasacchi<sup>1,4</sup> David B. Lindell<sup>1,2</sup> Sergey Tulyakov<sup>3</sup>  
<sup>1</sup>University of Toronto <sup>2</sup>Vector Institute <sup>3</sup>Snap Inc. <sup>4</sup>SFU

<https://snap-research.github.io/vd3d>



Figure 1: **3D camera control for text-to-video generation.** We introduce a method that can control camera poses for text-to-video generation using video diffusion transformers. (left) The method takes as input a set of camera poses used to generate each frame of a rendered video. (center, right) Applying multiple camera trajectories with the same text prompt enables synthesis of complex scenes from varied set of viewpoints.

## Abstract

Modern text-to-video synthesis models demonstrate coherent, photorealistic generation of complex videos from a text description. However, most existing models lack fine-grained control over camera movement, which is critical for downstream applications related to content creation, visual effects, and 3D vision. Recently, new methods demonstrate the ability to generate videos with controllable camera poses—these techniques leverage pre-trained U-Net-based diffusion models that explicitly disentangle spatial and temporal generation. Still, no existing approach enables camera control for new, transformer-based video diffusion models that process spatial and temporal information jointly. Here, we propose to tame video transformers for 3D camera control using a ControlNet-like conditioning mechanism that incorporates spatiotemporal camera embeddings based on Plucker coordinates. The approach demonstrates state-of-the-art performance for controllable video generation after fine-tuning on the RealEstate10K dataset. To the best of our knowledge, our work is the first to enable camera control for transformer-based video diffusion models.

## 1 Introduction

Text-to-video foundation models achieve unprecedented visual quality [7, 52]. They are trained on massive collections of images and videos and learn to synthesize remarkably consistent and physically plausible visualizations of the world. Yet, they lack built-in mechanisms for explicit 3D control during the synthesis process, requiring users to manipulate outputs through prompt engineering and

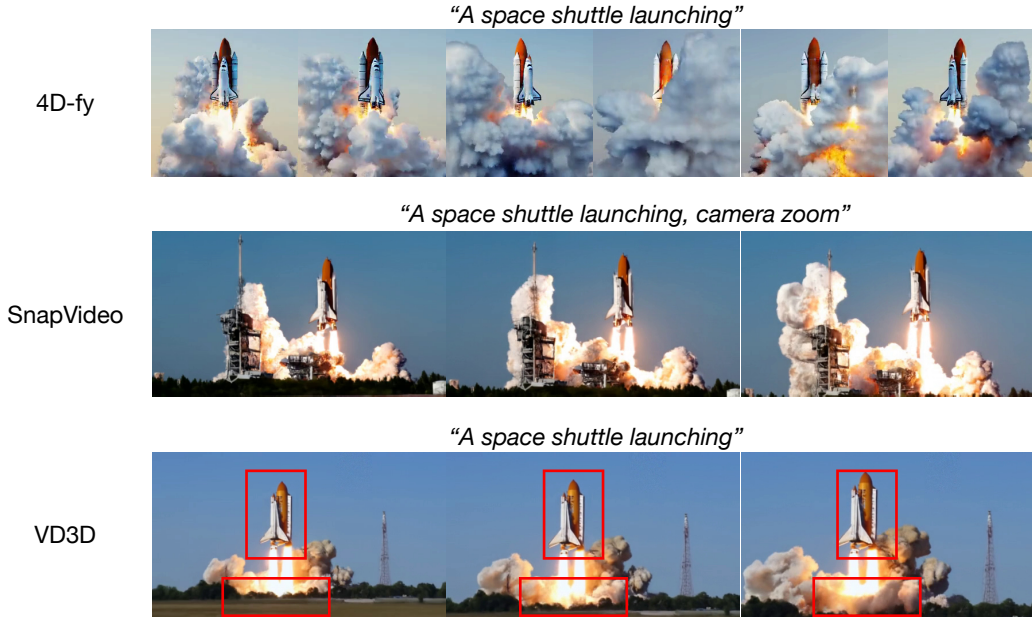


Figure 2: **Comparing text-to-video, text-to-4D, and camera-conditioned text-to-video generation.** Text-to-4D approaches, such as 4D-fy [3] (top) have full control over camera through use of a 3D representation, but they lack photorealism. (middle) Methods for text-to-video generation [41] create realistic videos, but do not provide explicit control over the viewpoint. In contrast, camera-conditioned text-to-video generation (bottom) bridges the gap between the two paradigms by extending text-to-video generators with 3D camera control without using an explicit 3D representation. Please see the supplementary webpage for the corresponding video results.

trial and error—a slow, laborious, and computationally expensive process. For example, as Fig. 2 shows, state-of-the-art video models struggle to follow even simple “zoom-in” or “zoom-out” camera trajectories using text prompt instructions (see supplemental webpage). This lack of controllability limits interactivity and makes existing video generation techniques challenging to use for artists or other end users. We augment 2D video generation models with control over the position and orientation of the camera, providing finer-grained control compared to text prompting, and facilitating use of video generation models for downstream applications.

Several contemporary works [65, 19, 78] propose methods for camera control of state-of-the-art, open-source video diffusion models. The key technical insight proposed by these methods is to add camera control by fine-tuning the temporal conditioning layers of a U-Net-based video generation model on a dataset with high-quality camera annotations. While these techniques achieve promising results, they are not applicable to more recent, high-quality transformer-based architectures [60, 46], such as Sora [7], SnapVideo [41], and Lumina-T2X [15], as these latest works simply do not have standalone temporal layers amenable to camera conditioning.

Large video transformers represent a video as a (possibly compressed) sequence of tokens, applying self-attention layers to all the tokens jointly [7, 41]. Consequently, they do not have standalone temporal layers, which are essential for current camera conditioning approaches to integrate viewpoint information, making them inapplicable to such models. As the community shifts towards large video transformers to jointly model spatiotemporal dependencies in the data, it is critical to develop methods that provide similar capabilities for camera control. Our work designs a camera conditioning method tailored to the joint spatiotemporal computation used in large video transformers and takes a step towards taming them for controllable video synthesis.

We develop our work on top of our implementation of SnapVideo [41], a state-of-the-art video diffusion model, that employs FIT-blocks [11] for efficient video modeling in the compressed latent space. We investigate various camera conditioning mechanisms in the fine-tuning scenario and explore trade-offs in terms of visual quality preservation and controllability. Our findings reveal

that simply adapting existing approaches to video transformers does not yield satisfactory results: they either enable some limited amount of control while reducing the visual quality of the output video, or they entirely fail to control camera motion. Our key technical insight is to enable the control through spatiotemporal camera embeddings, which we derive by combining Plucker coordinates with the network input through a separately trained cross-attention layer. To the best of our knowledge, our work is the first to explore a ControlNet-like [89] conditioning mechanism for spatiotemporal transformers.

We evaluate the method on a collection of manually crafted text prompts and unseen camera trajectories and compare to baseline approaches that incorporate previous camera control methods into a video transformer. Our approach achieves state-of-the-art results in terms of camera controllability and video quality, and also enables downstream applications such as multi-view, text-to-video generation, as depicted in Fig. 1. In contrast to existing image-to-3D methods (e.g., [39, 48, 61]), which are limited to object-centric scenes, our approach synthesizes novel views for real input images with complex environments.

Overall, our work makes the following contributions.

- We propose a new method to tame large video transformers for 3D camera control. Our approach uses a ControlNet-like conditioning mechanism that incorporates spatiotemporal camera embeddings based on Plucker coordinates.
- We thoroughly evaluate this approach, including comparisons to previous camera control methods, which we adapt to the video transformer architecture.
- We demonstrate state-of-the-art results in controllable video generation by applying the proposed conditioning method and fine-tuning scheme to the SnapVideo model [41].

## 2 Related work

Our method is connected to techniques related to text-to-video, text-to-3D, and text-to-4D generation. As this is a popular and fast-moving field, this section provides only a partial overview with a focus on the most relevant techniques; we refer readers to Po et al. [47] and Yunus et al. [85] for a more thorough review of related techniques.

**Text-to-video generation.** Our work builds on recent developments in 2D video generation models. One such class of these techniques works by augmenting text-to-image models with layers that operate on the temporal dimension to facilitate video generation [6, 53, 69, 18, 5]. Video generation methods can be trained in a hybrid fashion on both images and video to improve the generation quality [4, 62, 76, 22, 18, 20, 63, 94]. While these techniques are primarily based on convolutional, U-Net-style architectures, a recent shift towards transformer-based models enables synthesis of much longer videos with significantly higher quality [7, 40, 41]. Still, these recent techniques do not enable synthesis with controllable camera motion.

**4D generation.** Previous methods also tackle the problem of 4D generation, i.e., generating videos of dynamic 3D scenes from controllable viewpoints, usually from an input text prompt or image. Since the initial work on this topic using large-scale generative models [54], significant improvements in the visual quality and motion quality of generated scenes have been achieved [50, 37, 3, 93, 16, 77, 28, 1, 90, 72, 42, 34]. While these methods generate scenes based on text conditioning, other approaches convert an input image or video to a dynamic 3D scene [50, 92, 81, 45, 93, 37, 16, 86, 12, 70, 79, 64, 14, 55, 87, 83, 51, 33, 35, 59, 58, 26, 8, 36, 88]. Another line of work [2, 75] extends 3D GANs into 4D by training on 2D videos, however the quality is limited and models are trained on single category datasets. Still, all of these methods are focused on object-centric generation, typically based on 3D volumetric representations. As such, they typically do not incorporate background elements, and overall, they do not approach the level of photorealism demonstrated by the state-of-the-art video generation models used in our technique.

**Controllable generation with diffusion models.** Methods for controllable generation using diffusion models have had significant impact, both in the context of image and video generation. For example, existing techniques allow controllable image generation conditioned on text, depth maps, edges, pose, or other signals [89, 80]. Furthermore, there is a line of work for 3D generation which conditions diffusion models on camera poses for view-consistent multi-view generation [66, 56, 9, 84, 32, 44, 17]. Our approach is most similar to related techniques in video generation that seek to control the camera

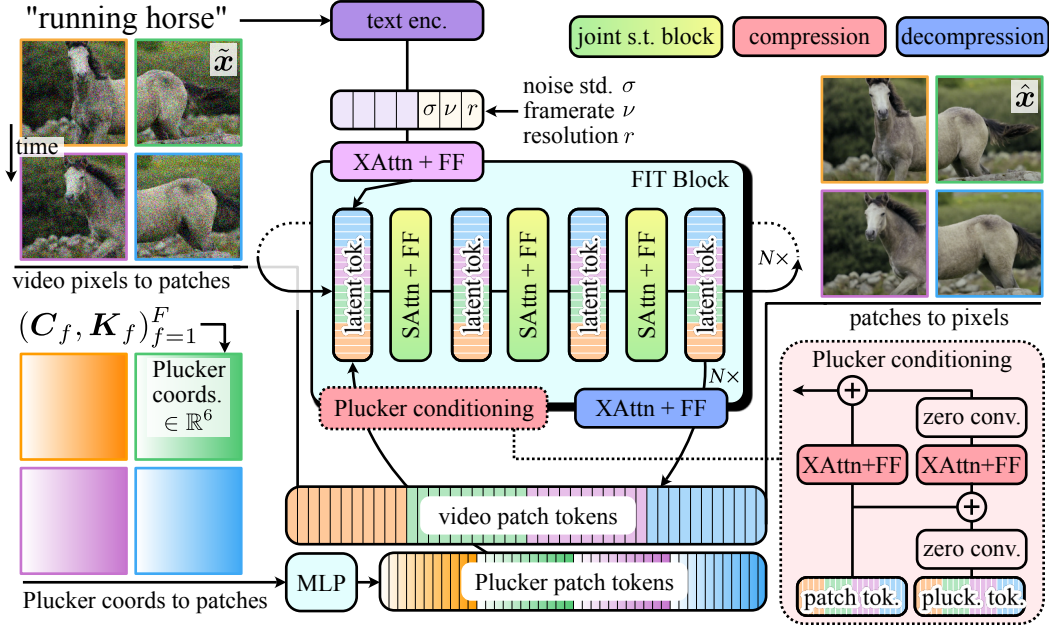


Figure 3: **Overview of architecture.** We adapt the Snap Video FIT architecture [41] to incorporate camera control. We take as input the noisy input video  $\tilde{x}$ , camera extrinsics  $C_f$ , and camera intrinsics  $K_f$  for each video frame  $f$ . Using the camera parameters, we compute the Plücker coordinates for each pixel within the video frames. Both the input video and Plücker coordinate frames are converted to patch tokens, and we condition the video patch tokens using a mechanism similar to ControlNet [89] (“Plücker conditioning” block). Then, the model estimates the denoised video  $\hat{x}$  by recurrent application of FIT blocks [11]. Each block reads information from the patch tokens into a small set of latent tokens on which computation is performed. The results are written to the patch tokens in an iterative denoising diffusion process.

position. For example, MotionCtrl [65] designs camera and object control mechanisms for the VideoCrafter1 [10] and SVD [5] models.

**Concurrent 3D camera control methods.** Concurrent approaches enable camera control by conditioning the temporal layers of the network with camera pose information, e.g., using Plücker coordinates [19, 18, 73, 31] or other embeddings [78]. Interestingly, it is also possible to incorporate camera control into video generation models without additional training through manipulation and masking of attention layers, though this requires additional tracking, segmentation, or depth for each input video [25, 71, 24]. Another recent work [38] transfers motion, including camera motion, to other generated videos.

Although these approaches demonstrate promising results for U-Net-based video diffusion models, the techniques are not applicable to modern video transformers that model spatio-temporal dynamics jointly. While another concurrent work [67] uses a transformer-based architecture for space and time, it does not tackle text-based generation for dynamic scenes but mainly novel view synthesis for 3D scenes. In our work, we design an efficient mechanism that enables camera control in video diffusion transformers using a ControlNet inspired mechanism without sacrificing visual quality.

### 3 Method

#### 3.1 Large text-to-video transformers

**Text-to-video generation.** Diffusion models have emerged as the dominant paradigm for large-scale video generation [23, 22, 7]. The standard setup considers the conditional distribution  $p(x|y)$  of videos  $x \in \mathbb{R}^{F \times H \times W}$  (consisting of  $F$  frames of  $H \times W$  resolution) given their textual descriptions  $y \in \mathcal{Y}^L$ , consisting of  $L$  (possibly padded) tokens from the alphabet  $\mathcal{Y}$ . Following [29], our



video diffusion framework assumes a denoising model  $D_\theta : (\tilde{\mathbf{x}}; \mathbf{y}, \sigma) \mapsto \hat{\mathbf{x}}$  that predicts a clean video  $\hat{\mathbf{x}}$  from the corresponding noised input  $\tilde{\mathbf{x}} = \mathbf{x} + \sigma\boldsymbol{\varepsilon}$ ,  $\sigma \in \mathbb{R}_+$ ,  $\boldsymbol{\varepsilon} \sim \mathcal{N}(\mathbf{0}, \mathbf{I})$ . The model is parametrized by a neural network  $F_\theta(\tilde{\mathbf{x}}; \mathbf{y}, \sigma)$  as  $D_\theta(\tilde{\mathbf{x}}; \mathbf{y}, \sigma) = c_{\text{out}}(\sigma)F_\theta(c_{\text{in}}(\sigma)\tilde{\mathbf{x}}; \mathbf{y}, \sigma) + c_{\text{skip}}(\sigma)\tilde{\mathbf{x}}$ . The optimization objective is defined as follows:

$$\mathcal{L}(\theta) \triangleq \mathbb{E}_{(\mathbf{x}, \mathbf{y}), \sigma, \boldsymbol{\varepsilon}} [\|D_\theta(\mathbf{x} + \sigma\boldsymbol{\varepsilon}; \mathbf{y}, \sigma) - \mathbf{x}\|_2^2] \longrightarrow \min_{\theta} \quad (1)$$

We refer a reader to [41] and [29] for further details on the diffusion setup, which we adopted without modifications.

**Spatiotemporal transformers.** Following SnapVideo [41], our video generator consists of two models: the base 4B-parameters generator, operating on 16-frames  $36 \times 64$  resolution videos, and a  $288 \times 512$  upsampler. The latter, a diffusion model itself, is fine-tuned from the base model and conditioned on the low-resolution videos. Each model uses FIT transformer blocks [11, 27] for efficient self-attention operations (see Fig. 3). An FIT model consists of  $B$  blocks (we have  $B = 6$  in all the experiments) and first partitions each frame in an input video into patches [13] of resolution  $h_p \times w_p$  (we use  $h_p = w_p = 4$  in all the experiments). These video patches are then independently projected via a feedforward (FF) layer to obtain a sequence of video tokens  $[\mathbf{v}_\ell]_{\ell=1}^L \triangleq (\mathbf{v}_1, \dots, \mathbf{v}_L) \in \mathbb{R}^{L \times d}$  of length  $L = F \times (H/h_p) \times (W/w_p)$  and dimensionality  $d$ . Next, each FIT block “reads” the information from this video sequence into a much shorter sequence of *latent* tokens  $[\mathbf{z}_m]_{m=1}^M \triangleq (\mathbf{z}_1, \dots, \mathbf{z}_M)$  through a “read” cross-attention layer, followed by a feedforward layer. The core processing with self-attention layers is performed in this latent space, and then the result is written back to the video tokens through a corresponding “write” cross-attention layer (also followed by an FF layer). The latent tokens in each next FIT block are initialized from the previous one, which helps to propagate the computational results throughout the network. In this way, the entire computation occurs jointly in both spatial and temporal axes, which yields superior scalability properties [41]. However, it abandons the decomposed spatial/temporal computation nature of modern video diffusion U-Nets, which is vital for modern camera conditioning techniques [65, 78] to enforce control without compromising visual quality.

### 3.2 Camera control for spatiotemporal transformers

**Spatiotemporal camera representation.** The standard way of representing camera parameters for a video (in the pinhole model) is via a trajectory of extrinsics and intrinsics camera parameters  $(\mathbf{C}_f, \mathbf{K}_f)_{f=1}^F$  for each  $f$ -th frame, where  $\mathbf{C}_f = [\mathbf{R}; \mathbf{t}] \in \mathbb{R}^{3 \times 4}$ , describes the camera rotation  $\mathbf{R} \in \mathbb{R}^{3 \times 3}$  and translation  $\mathbf{t} \in \mathbb{R}^3$ , and  $\mathbf{K}_f \in \mathbb{R}^{3 \times 3}$  contains the focal length and principal point (and also horizontal/vertical skew coefficient, but it is always 0 in our setup). To control camera motion, existing methods such as [65, 78, 25] condition the temporal attention layers of U-Net-based video generators on embeddings computed from these camera parameters. Such a pipeline provides a good conditioning signal for convolutional video generators with decomposed spatial/temporal computation, but our experiments demonstrate that it works poorly for spatiotemporal transformers: they either fail to pick up any controllability (when being added as transformed residuals to the latent tokens), or degrade the visual quality of the output (when the original network parameters are being fine-tuned). This motivates us to design a better camera conditioning scheme, tailored for modern large-scale spatiotemporal transformers.

First, we propose to normalize the camera parameters to the very first frame, forcing the first frame’s rotation be an identity matrix  $\mathbf{R}_1 = \mathbf{I}$  and translation be zero:  $\mathbf{t}_1 = \mathbf{0}$ . We then recompute the extrinsics for each  $f$ -th frame as  $\mathbf{C}_f = [\mathbf{R}_1^{-1}\mathbf{R}_f; \mathbf{t}_f - \mathbf{t}_1]$ , establishing a consistent coordinate system across videos. After that, we found it essential to enrich the conditioning information by switching from temporal frame-level camera parameters to pixel-wise *spatiotemporal* camera parameters. This is achieved by computing the Plücker coordinates for each pixel, providing fine-grained positional representation.

Plücker coordinates provide a convenient parametrization of lines in the 3D space, and we use them to compute fine-grained positional representations of each pixel in each frame of a video. Given the extrinsic and intrinsic camera parameters  $\mathbf{R}, \mathbf{t}, \mathbf{K}_f$  of the  $f$ -th frame, we parametrize each  $(h, w)$ -th pixel as a Plücker embedding  $\ddot{\mathbf{p}}_{f,h,w} \in \mathbb{R}^6$  from the camera position to the pixel’s center as

$$\ddot{\mathbf{p}}_{f,h,w} = (\mathbf{t}_f \times \hat{\mathbf{d}}_{f,h,w}, \hat{\mathbf{d}}_{f,h,w}), \quad \hat{\mathbf{d}}_{f,h,w} = \frac{\mathbf{d}}{\|\mathbf{d}_{f,h,w}\|}, \quad \mathbf{d}_{f,h,w} = \mathbf{R}_f \mathbf{K}_f [w, h, 1]^\top + \mathbf{t}_f. \quad (2)$$

This approach mirrors the technique used in CameraCtrl [19], a concurrent study focusing on camera control in U-Net-based video diffusion models. The motivation for using Plücker coordinates is that geometric manipulations in the Plücker space can be performed through simple arithmetics on the coordinates, which makes it easier for the network to use the positional information stored in such a disentangled representation.

Computing Plücker coordinates for each pixel results in a  $\ddot{\mathbf{P}} \in \mathbb{R}^{6 \times F \times H \times W}$  spatiotemporal camera representation for a video. To input it into the model, we first perform the equivalent ViT-like [13]  $h_p \times w_p$  patchification procedure. It is followed by a learnable feedforward layer  $\text{FF}_{\ddot{p}}$  to obtain the Plücker camera tokens sequence  $[\ddot{c}_\ell]_{\ell=1}^L \in \mathbb{R}^{L \times d}$  of the same length  $L = F \times (H/h_p) \times (W/w_p)$  and dimensionality  $d$  as the video tokens sequence  $[\mathbf{v}_\ell]_{\ell=1}^L$ . This spatiotemporal representation carries fine-grained positional information about each pixel in a video, making it easier for the generator to accurately follow the desired camera motion.

**Camera conditioning.** To input the rich spatiotemporal camera information in the form of Plücker embeddings into our video generator, we design an efficient ControlNet like [89] mechanism tailored for large transformer models (see Fig. 3). This mechanism is guided by two main objectives: 1) the model should be amenable to rapid fine-tuning from a small dataset with estimated camera positions; and 2) the visual quality shouldn’t be compromised during the fine-tuning stage. We found that meeting these objectives is more challenging for spatiotemporal transformers compared to U-Net-based models with decomposed spatial/temporal computation, since even minor interventions into their design quickly lead to degraded video outputs. We hypothesize that the core reason for it is the entangled spatial/temporal computation of video transformers: any attempt to alter the temporal dynamics (such as camera motion) influences spatial communication between the tokens, leading to unnecessary signal propagation and overfitting during the fine-tuning stage. To mitigate this, we input the camera information gradually through read cross-attention layers, zero-initialized from the original network parameters of the corresponding layers.

Specifically, in each  $b$ -th FIT block of our video generator, we replace its standard read cross-attention operation (see [27, 41] for details):

$$[\mathbf{z}_m^{(b)}]_{m=1}^M = \text{FF}^{(b)}(\text{XAttn}^{(b)}([\mathbf{z}_m^{(b)}]_{m=1}^M, [\mathbf{v}_\ell^{(b)}]_{\ell=1}^L)), \quad (3)$$

where  $\text{FF}(\cdot)$  and  $\text{XAttn}(\cdot, \cdot)$  denote feed-forward and cross-attention layers respectively, with:

$$[\mathbf{z}_m^{(b)}]_{m=1}^M = \text{FF}^{(b)}(\text{XAttn}^{(b)}([\mathbf{z}_m^{(b)}]_{m=1}^M, [\mathbf{v}_\ell^{(b)}]_{\ell=1}^L)) \quad (4)$$

$$+ \text{Conv}_{\text{res}}^{(b)}(\text{FF}_{\text{cam}}^{(b)}(\text{XAttn}_{\text{cam}}^{(b)}([\mathbf{z}_m^{(b)}]_{m=1}^M, \text{Conv}_{\text{plück}}^{(b)}([\ddot{c}_\ell]_{\ell=1}^L)))). \quad (5)$$

where  $\text{FF}_{\text{cam}}^{(b)}$ , and  $\text{XAttn}_{\text{cam}}^{(b)}$  are learnable layers, and  $\text{Conv}_{\text{plück}}^{(b)}$ ,  $\text{Conv}_{\text{res}}^{(b)}$  are 1-dimensional convolutions that process plucker camera tokens and their final representations inside, respectively. It is crucial to instantiate the weights of these convolutions from zeros to preserve the model initialization. Besides, we initialize the weights of  $\text{FF}_{\text{cam}}^{(b)}$  and  $\text{XAttn}_{\text{cam}}^{(b)}$  from the corresponding parameters of the original network. This approach helps to preserve visual quality at initialization and facilitates rapid fine-tuning on a small dataset. As a result, we obtain the method for fine-grained 3D camera control in large video diffusion transformers. We name it VD3D and visualize its architecture in Fig. 3.

### 3.3 Training details

**Optimization details.** To ensure comparability with prior work such as [65], we train our video generator on the same RealEstate10k dataset [95]. We optimize only the newly added parameters  $\text{FF}_{\ddot{p}}$  and  $(\alpha^{(b)}, \text{FF}^{(b)}, \text{XAttn}^{(b)})_{b=1}^B$ , and keep the rest of the network frozen. We found that training only the base  $36 \times 64$  model was sufficient, as the  $288 \times 512$  upsampler already accurately follows the camera motion of a low-resolution video. We experiment with two model variants: a smaller generator with approximately 700 million parameters for ablations and initial explorations, and a larger 4 billion parameter model, which we use for the main results in this paper. Both models were trained with a batch size of 256 over 50,000 optimization steps with the LAMB optimizer [82]. The learning rate was warmed up for the first 10,000 iterations from 0 to 0.005 and then linearly decreased to 0.0015 over subsequent iterations. Since the original video diffusion model is trained in the any-frame-conditioning pipeline [41], we can produce variable camera trajectories from the same starting frame. For text conditioning, we use the T5-11B [49] language model to encode

text 1024-dimensional embeddings into 128-length sequences. For training efficiency, they were precomputed for the entire dataset. The rest of the training details have been adopted from [41].

**Compute details.** A single training run for the smaller 700M parameter generator takes approximately 1 day on a node equipped with  $8 \times$  NVIDIA A100 40GB GPUs, connected via NVIDIA NVLink, along with 960 GB of RAM and 92 Intel Xeon CPUs. The larger 4B parameter model was trained on 8 such nodes for 1,5 days, totaling  $64 \times$  NVIDIA A100 40GB GPUs. In total, we conducted  $\approx 150$  training runs for the smaller model during the development stage of 4B generator. Consequently, the project’s total compute utilization amounted to approximately 2700 NVIDIA A100 40GB GPU-days.

### 3.4 Dataset

We fine-tune the pre-trained text-to-video model (SnapVideo [41]), on RealEstate10K [95]. The training split consists of roughly 65K video clips, and is the same as is used in concurrent work (MotionCtrl [65] and CameraCtrl [19]). We evaluate our method using 20 camera trajectories sampled from the RealEstate10K test split that were not seen during training for the user study. For the automated evaluations, we use the full test split.

### 3.5 Metrics

We conduct a user study to evaluate our approach for camera-controlled text-to-video generation. The study participants are presented with 20 side-by-side comparisons between the proposed approach and the baselines as well as a reference video from RealEstate10K with the same trajectory to better judge the camera alignment. We ask 20 participants for each generated video sequence to indicate which generated video they prefer based on multiple submetrics, namely, camera alignment, motion quality, text alignment, visual quality, and overall preference. The user study involved negligible risk to the participants and was conducted with appropriate institutional review board and legal approval. Participants were compensated 0.30 USD per question.

### 3.6 Baselines

We compare our work to the two concurrent works MotionCtrl [65] and CameraCtrl [19] by adapting their publicly released code to the SnapVideo model [41]. Note that both baselines were originally designed for space-time disentangled U-Net video diffusion models. Hence, their approaches are not directly applicable to the spatio-temporal transformers, and so we adapt them to this setting as follows. For MotionCtrl, we omit their object motion control module and use their proposed camera motion control module to encode the camera parameters into a context vector used with the SnapVideo model. We fine-tune both the camera motion control module and the cross attention between the latent vectors and the patches. We also train one version of MotionCtrl where we freeze the original base model to prevent quality degradation. For CameraCtrl, we fine-tune the original camera encoder module and use this to produce the latent vectors in the SnapVideo model. During fine-tuning the model weights are kept frozen—i.e., the same as in our proposed approach.

## 4 Experiments

### 4.1 Assessment

We provide a qualitative and quantitative assessment of our approach compared to the baselines in Fig. 4 and in Tab. 1. Following CameraCtrl [19], we also evaluate the camera pose accuracy using ParticleSfM [91] on generated videos in Tab. 2. We using generations for text prompts from RealEstate10K [95] and MSR-VTT [74], testing both in- and out-of-distribution prompts. Note that we adjust the CameraCtrl [19] evaluation pipeline by normalizing all cameras into a unified scale as COLMAP provides different scales across different scenes. This prevents scenes with large scale to have a higher impact on the errors. Please also refer to the supplementary webpage for additional video results.

In Fig. 4 we observe that adapting the camera conditioning method from the MotionCtrl degrades visual quality and text alignment, likely because this approach adjusts the weights of the base video model. In the space-time U-Net for which this approach was proposed, the temporal layers can be

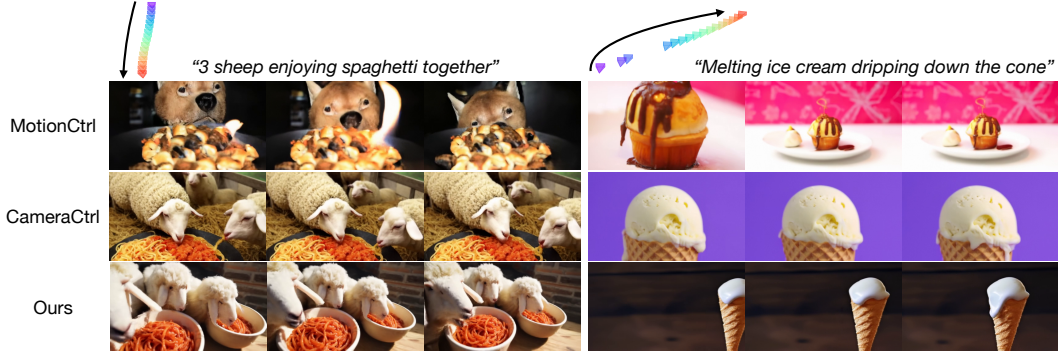


Figure 4: **Camera-conditioned text-to-video generation.** Comparison of the proposed approach to MotionCtrl and CameraCtrl for the same camera trajectory input. MotionCtrl exhibits worse quality due to fine-tuning of existing layers and CameraCtrl is not sensitive to camera conditioning. See the supplementary webpage for video results.

Table 1: **Quantitative results.** We compare our method to MotionCtrl and CameraCtrl implemented on the same base video models as ours. The methods are evaluated in a user study in which participants indicate their preference based on camera alignment (CA), motion quality (MQ), text alignment (TA), visual quality (VQ), and overall preference (Overall). The percentages indicate preference for VD3D vs. the alternative method (in each row). All results are statistically significant with  $p < 0.001$  as evaluated using a  $\chi^2$  test.

Method	Human Preference				
	CA	MQ	TA	VQ	Overall
VD3D vs. MotionCtrl	82%	81%	86%	81%	84%
VD3D vs. CameraCtrl	78%	64%	63%	65%	66%

fine-tuned without sacrificing visual fidelity. Since spatio-temporal transformers do not decompose temporal and spatial attributes in the same way, the model overfits to the small dataset used to fine-tune the cross-attention layer. While we observe some agreement with the camera poses used to condition the model, the text alignment is generally low in our experiments (see supplemental webpage). In contrast, CameraCtrl keeps the pre-trained video model weights frozen and only trains a camera encoder. This leads to strong visual quality, but the generated videos show little agreement with the input camera poses. We hypothesize that this is due random initialization of the new temporal attention layers and convolutions. For fair comparison, we trained all models for the same number of iterations (described in Sec. 3.3). We believe that CameraCtrl requires substantially longer training time to converge in comparison to our ControlNet-inspired conditioning mechanism (see the Plucker conditioning module in Fig. 3), which is initialized using a copy of the cross-attention and feed-forward layer and fine-tuned.

The results of the user study in Tab. 1 show that most participants prefer the generated videos using the proposed camera conditioning mechanism across all evaluated sub-metrics. We also observe a pronounced preference for the camera alignment of the proposed method compared to the other baselines. That is, 82% and 78% of participants prefer the camera alignment of the proposed method compared to our respective adaptations of MotionCtrl and CameraCtrl to the video transformer model. All results are significant at the  $p < 0.001$  level as evaluated using a  $\chi^2$  test.

## 4.2 Ablations

**Plucker embedding.** We motivate our Plucker embedding conditioning mechanism by training a variant using the raw camera matrices. Concretely, we flatten and concatenate extrinsics and intrinsics matrices in the channel dimension and repeat the values in the spatial patch dimensions. We observe that Plucker embeddings provide an essential spatial conditioning mechanism, as shown in Tab. 2.

Table 2: **Camera pose evaluation.** We evaluate all models using reference camera trajectories from the RealEstate10K test set. We compute translation and rotation errors based on estimated camera poses from generations using ParticleSfM [91].

Method	RealEstate10K		MSR-VTT	
	TransError ( $\downarrow$ )	RotError ( $\downarrow$ )	TransError ( $\downarrow$ )	RotError ( $\downarrow$ )
Base Model	0.616	0.207	0.717	0.216
MotionCtrl	0.518	0.161	0.627	0.148
MotionCtrl (frozen)	0.607	0.205	0.678	0.122
CameraCtrl	0.532	0.165	0.578	0.220
Ours	<b>0.409</b>	<b>0.043</b>	<b>0.504</b>	<b>0.050</b>
w/o Plucker	0.517	0.161	0.676	0.156
w/o ControlNet	0.573	0.182	0.787	0.179
w/o weight copy	0.424	0.044	0.513	0.063

**ControlNet conditioning.** Our ControlNet inspired conditioning mechanism ensures fast and precise learning of the conditioning signal distribution. Instead of using a ControlNet block, we simply add zero-initialized Plucker embedding features to the patches and observe close to no camera control. We observe training cross-attention layers in the ControlNet block is key to learning camera control while preserving the original model weights. This is confirmed by our camera evaluation in Tab. 2.

**ControlNet weight copy.** While the ControlNet block is essential, copying the pre-trained weights into the new copy has rather minor impact, as shown in Tab. 2. To verify this, we train a model where we randomly initialize the cross-attention block between patches and latents instead of copying the weights. We observe similar results, showing that rather the architecture and zero-initialization are the key component of this design.

### 4.3 Applications

**Image-to-video generation.** We synthesize camera-controlled videos based on different camera poses as shown in Fig. 1. For this task we use a version of the SnapVideo model that we fine-tune on video sequences where a random subset of the input frames are masked. At inference time, we can provide image guidance for any of the generated frames, providing an additional dimension of controllability when paired with our proposed method for camera control. To demonstrate image-to-video generation in Fig. 1, we condition the model using camera poses along with image guidance from the first frame of a generated video sequence. Note that our method provides no control over motion within the scene itself; hence, scene motion can differ depending on the random seed or the provided camera poses.

**Image-to-multiview generation.** We also explore multi-view generation for static scenes as shown in Fig. 5. Given a real input image of a complex scene unseen during training, our camera-conditioned model generates view-consistent renderings of that scene from arbitrary viewpoints. These multi-view renderings could be directly relevant to downstream 3D reconstructions pipelines, e.g., based on NeRF [43] or 3D Gaussian Splatting [30]. We show the potential of camera-conditioned image-to-multiview generation for complex 3D scene generation, but we leave more extensive exploration of this topic for future work.

## 5 Conclusion

Large-scale video transformer models show immense promise to solve many long-standing challenges in computer vision, including novel-view synthesis, single-image 3D reconstruction, and text-conditioned scene synthesis. Our work brings additional controllability to these models, enabling a user to specify the camera poses from which video frames are rendered.

**Limitations and future work.** There are several limitations to our work, which highlight important future research directions. For example, while rendering static scenes from different camera view-





Figure 5: **Conditional multi-view generation on a real image.** We can generate arbitrary camera trajectories from a given real image for multi-view synthesis, paving the way to single-image scene reconstruction using camera-controlled video models.

points produces results that appear 3D consistent, dynamic scenes rendered from different camera viewpoints can have inconsistent motion (see supplemental videos). We envision that future video generation models will have fine-grained control over both scene motion and camera motion to address this issue. Further, our approach applies camera conditioning only to the low-resolution SnapVideo model and we keep their upsampler model frozen (i.e., without camera conditioning)—it may be possible to further improve camera control through joint training, though this brings additional architectural engineering and computational challenges. Finally, our approach is currently limited to generation of relatively short videos (16 frames), based on the design and training scheme of the SnapVideo model. Future work to address these limitations will enable new capabilities for applications in computer vision, visual effects, augmented and virtual reality, and beyond.

**Broader impacts.** Recent video generation models demonstrate coherent, photorealistic synthesis of complex scenes—capabilities that are highly sought after for numerous applications across computer vision, graphics, and beyond. Our key technical contributions relate to camera control of these models, which can be applied to a wide range of methods. As with all generative models and technologies, underlying technologies can be misused by bad actors in unintended ways. While these methods continue to improve, researchers and developers should continue to consider safeguards, such as output filtering, watermarking, access control, and others.

## References

- [1] Sherwin Bahmani, Xian Liu, Wang Yifan, Ivan Skorokhodov, Victor Rong, Ziwei Liu, Xihui Liu, Jeong Joon Park, Sergey Tulyakov, Gordon Wetzstein, Andrea Tagliasacchi, and David B. Lindell. Tc4d: Trajectory-conditioned text-to-4d generation. In *Proc. ECCV*, 2024.
- [2] Sherwin Bahmani, Jeong Joon Park, Despoina Paschalidou, Hao Tang, Gordon Wetzstein, Leonidas Guibas, Luc Van Gool, and Radu Timofte. 3d-aware video generation. In *TMLR*, 2023.
- [3] Sherwin Bahmani, Ivan Skorokhodov, Victor Rong, Gordon Wetzstein, Leonidas Guibas, Peter Wonka, Sergey Tulyakov, Jeong Joon Park, Andrea Tagliasacchi, and David B. Lindell. 4d-fy: Text-to-4d generation using hybrid score distillation sampling. In *Proc. CVPR*, 2024.
- [4] Max Bain, Arsha Nagrani, Gül Varol, and Andrew Zisserman. Frozen in time: A joint video and image encoder for end-to-end retrieval. In *Proc. ICCV*, 2021.
- [5] Andreas Blattmann, Tim Dockhorn, Sumith Kulal, Daniel Mendelevitch, Maciej Kilian, Dominik Lorenz, Yam Levi, Zion English, Vikram Voleti, Adam Letts, et al. Stable video diffusion: Scaling latent video diffusion models to large datasets. *arXiv preprint arXiv:2311.15127*, 2023.
- [6] Andreas Blattmann, Robin Rombach, Huan Ling, Tim Dockhorn, Seung Wook Kim, Sanja Fidler, and Karsten Kreis. Align your latents: High-resolution video synthesis with latent diffusion models. In *Proc. CVPR*, 2023.

- [7] Tim Brooks, Bill Peebles, Connor Holmes, Will DePue, Yufei Guo, Li Jing, David Schnurr, Joe Taylor, Troy Luhman, Eric Luhman, Clarence Ng, Ricky Wang, and Aditya Ramesh. Video generation models as world simulators. *OpenAI technical reports*, 2024.
- [8] Zenghao Chai, Chen Tang, Yongkang Wong, and Mohan Kankanhalli. Star: Skeleton-aware text-based 4d avatar generation with in-network motion retargeting. *arXiv preprint arXiv:2406.04629*, 2024.
- [9] Eric R Chan, Koki Nagano, Matthew A Chan, Alexander W Bergman, Jeong Joon Park, Axel Levy, Miika Aittala, Shalini De Mello, Tero Karras, and Gordon Wetzstein. Generative novel view synthesis with 3d-aware diffusion models. In *Proc. ICCV*, 2023.
- [10] Haoxin Chen, Menghan Xia, Yingqing He, Yong Zhang, Xiaodong Cun, Shaoshu Yang, Jinbo Xing, Yaofang Liu, Qifeng Chen, Xintao Wang, Chao Weng, and Ying Shan. Videocrafter1: Open diffusion models for high-quality video generation. *arXiv preprint arXiv:2310.19512*, 2023.
- [11] Ting Chen and Lala Li. Fit: Far-reaching interleaved transformers. *arXiv preprint arXiv:2305.12689*, 2023.
- [12] Wen-Hsuan Chu, Lei Ke, and Katerina Fragkiadaki. Dreamscene4d: Dynamic multi-object scene generation from monocular videos. *arXiv preprint arXiv:2405.02280*, 2024.
- [13] Alexey Dosovitskiy, Lucas Beyer, Alexander Kolesnikov, Dirk Weissenborn, Xiaohua Zhai, Thomas Unterthiner, Mostafa Dehghani, Matthias Minderer, Georg Heigold, Sylvain Gelly, et al. An image is worth 16x16 words: Transformers for image recognition at scale. *Proc. ICLR*, 2021.
- [14] Yutao Feng, Yintong Shang, Xiang Feng, Lei Lan, Shandian Zhe, Tianjia Shao, Hongzhi Wu, Kun Zhou, Hao Su, Chenfanfu Jiang, et al. Elastogen: 4d generative elastodynamics. *arXiv preprint arXiv:2405.15056*, 2024.
- [15] Peng Gao, Le Zhuo, Ziyi Lin, Dongyang Liu, Ruoyi Du, Xu Luo, Longtian Qiu, Yuhang Zhang, et al. Lumina-t2x: Transforming text into any modality, resolution, and duration via flow-based large diffusion transformers. *arXiv preprint arXiv:2405.05945*, 2024.
- [16] Quankai Gao, Qiangeng Xu, Zhe Cao, Ben Mildenhall, Wenchao Ma, Le Chen, Danhang Tang, and Ulrich Neumann. Gaussianflow: Splatting Gaussian dynamics for 4D content creation. *arXiv preprint arXiv:2403.12365*, 2024.
- [17] Ruiqi Gao, Aleksander Holynski, Philipp Henzler, Arthur Brussee, Ricardo Martin-Brualla, Pratul Srinivasan, Jonathan T Barron, and Ben Poole. Cat3d: Create anything in 3d with multi-view diffusion models. *arXiv preprint arXiv:2405.10314*, 2024.
- [18] Yuwei Guo, Ceyuan Yang, Anyi Rao, Yaohui Wang, Yu Qiao, Dahua Lin, and Bo Dai. Animatediff: Animate your personalized text-to-image diffusion models without specific tuning. *Proc. ICLR*, 2024.
- [19] Hao He, Yinghao Xu, Yuwei Guo, Gordon Wetzstein, Bo Dai, Hongsheng Li, and Ceyuan Yang. Cameractrl: Enabling camera control for text-to-video generation. *arXiv preprint arXiv:2404.02101*, 2024.
- [20] Yingqing He, Tianyu Yang, Yong Zhang, Ying Shan, and Qifeng Chen. Latent video diffusion models for high-fidelity video generation with arbitrary lengths. *arXiv preprint arXiv:2211.13221*, 2022.
- [21] Martin Heusel, Hubert Ramsauer, Thomas Unterthiner, Bernhard Nessler, and Sepp Hochreiter. Gans trained by a two time-scale update rule converge to a local nash equilibrium. *Proc. NeurIPS*, 2017.
- [22] Jonathan Ho, William Chan, Chitwan Saharia, Jay Whang, Ruiqi Gao, Alexey Gritsenko, Diederik P Kingma, Ben Poole, Mohammad Norouzi, David J Fleet, et al. Imagen video: High definition video generation with diffusion models. *arXiv preprint arXiv:2210.02303*, 2022.

- [23] Jonathan Ho, Tim Salimans, Alexey Gritsenko, William Chan, Mohammad Norouzi, and David J Fleet. Video diffusion models. *Proc. NeurIPS*, 2022.
- [24] Chen Hou, Guoqiang Wei, Yan Zeng, and Zhibo Chen. Training-free camera control for video generation. *arXiv preprint arXiv:2406.10126*, 2024.
- [25] Teng Hu, Jiangning Zhang, Ran Yi, Yating Wang, Hongrui Huang, Jieyu Weng, Yabiao Wang, and Lizhuang Ma. Motionmaster: Training-free camera motion transfer for video generation. *arXiv preprint arXiv:2404.15789*, 2024.
- [26] Tianyu Huang, Yihan Zeng, Hui Li, Wangmeng Zuo, and Rynson WH Lau. Dreamphysics: Learning physical properties of dynamic 3d gaussians with video diffusion priors. *arXiv preprint arXiv:2406.01476*, 2024.
- [27] Allan Jabri, David Fleet, and Ting Chen. Scalable adaptive computation for iterative generation. *arXiv preprint arXiv:2212.11972*, 2022.
- [28] Yanqin Jiang, Li Zhang, Jin Gao, Weimin Hu, and Yao Yao. Consistent4d: Consistent 360  $\{\deg\}$  dynamic object generation from monocular video. *Proc. ICLR*, 2024.
- [29] Tero Karras, Miika Aittala, Timo Aila, and Samuli Laine. Elucidating the design space of diffusion-based generative models. *Proc. NeurIPS*, 2022.
- [30] Bernhard Kerbl, Georgios Kopanas, Thomas Leimkühler, and George Drettakis. 3d gaussian splatting for real-time radiance field rendering. *Proc. ACM TOG*, 2023.
- [31] Zhengfei Kuang, Shengqu Cai, Hao He, Yinghao Xu, Hongsheng Li, Leonidas Guibas, and Gordon Wetzstein. Collaborative video diffusion: Consistent multi-video generation with camera control. *arXiv preprint arXiv:2405.17414*, 2024.
- [32] Nupur Kumari, Grace Su, Richard Zhang, Taesung Park, Eli Shechtman, and Jun-Yan Zhu. Customizing text-to-image diffusion with camera viewpoint control. *arXiv preprint arXiv:2404.12333*, 2024.
- [33] Yao-Chih Lee, Yi-Ting Chen, Andrew Wang, Ting-Hsuan Liao, Brandon Y Feng, and Jia-Bin Huang. Vividdream: Generating 3d scene with ambient dynamics. *arXiv preprint arXiv:2405.20334*, 2024.
- [34] Bing Li, Cheng Zheng, Wenxuan Zhu, Jinjie Mai, Biao Zhang, Peter Wonka, and Bernard Ghanem. Vivid-zoo: Multi-view video generation with diffusion model. *arXiv preprint arXiv:2406.08659*, 2024.
- [35] Renjie Li, Panwang Pan, Bangbang Yang, Dejia Xu, Shijie Zhou, Xuanyang Zhang, Zeming Li, Achuta Kadambi, Zhangyang Wang, and Zhiwen Fan. 4k4dgen: Panoramic 4d generation at 4k resolution. *arXiv preprint arXiv:2406.13527*, 2024.
- [36] Hanwen Liang, Yuyang Yin, Dejia Xu, Hanxue Liang, Zhangyang Wang, Konstantinos N Plataniotis, Yao Zhao, and Yunchao Wei. Diffusion4d: Fast spatial-temporal consistent 4d generation via video diffusion models. *arXiv preprint arXiv:2405.16645*, 2024.
- [37] Huan Ling, Seung Wook Kim, Antonio Torralba, Sanja Fidler, and Karsten Kreis. Align your gaussians: Text-to-4d with dynamic 3d gaussians and composed diffusion models. In *Proc. CVPR*, 2024.
- [38] Pengyang Ling, Jiazi Bu, Pan Zhang, Xiaoyi Dong, Yuhang Zang, Tong Wu, Huaian Chen, Jiaqi Wang, and Yi Jin. Motionclone: Training-free motion cloning for controllable video generation. *arXiv preprint arXiv:2406.05338*, 2024.
- [39] Minghua Liu, Chao Xu, Haian Jin, Linghao Chen, Mukund Varma T, Zexiang Xu, and Hao Su. One-2-3-45: Any single image to 3d mesh in 45 seconds without per-shape optimization. *Proc. NeurIPS*, 2024.
- [40] Xin Ma, Yaohui Wang, Gengyun Jia, Xinyuan Chen, Ziwei Liu, Yuan-Fang Li, Cunjian Chen, and Yu Qiao. Latte: Latent diffusion transformer for video generation. *arXiv preprint arXiv:2401.03048*, 2024.

- [41] Willi Menapace, Aliaksandr Siarohin, Ivan Skorokhodov, Ekaterina Deyneka, Tsai-Shien Chen, Anil Kag, Yuwei Fang, Aleksei Stoliar, Elisa Ricci, Jian Ren, et al. Snap video: Scaled spatiotemporal transformers for text-to-video synthesis. *Proc. CVPR*, 2024.
- [42] Qiaowei Miao, Yawei Luo, and Yi Yang. Pla4d: Pixel-level alignments for text-to-4d gaussian splatting. *arXiv preprint arXiv:2405.19957*, 2024.
- [43] Ben Mildenhall, Pratul P Srinivasan, Matthew Tancik, Jonathan T Barron, Ravi Ramamoorthi, and Ren Ng. Nerf: Representing scenes as neural radiance fields for view synthesis. In *Proc. ECCV*, 2020.
- [44] Norman Müller, Katja Schwarz, Barbara Rössle, Lorenzo Porzi, Samuel Rota Bulò, Matthias Nießner, and Peter Kotschieder. Multidiff: Consistent novel view synthesis from a single image. In *Proc. CVPR*, 2024.
- [45] Zijie Pan, Zeyu Yang, Xiatian Zhu, and Li Zhang. Fast dynamic 3d object generation from a single-view video. *arXiv preprint arXiv:2401.08742*, 2024.
- [46] William Peebles and Saining Xie. Scalable diffusion models with transformers. *Proc. ICCV*, 2023.
- [47] Ryan Po, Wang Yifan, Vladislav Golyanik, Kfir Aberman, Jonathan T Barron, Amit H Bermano, Eric Ryan Chan, Tali Dekel, Aleksander Holynski, Angjoo Kanazawa, et al. State of the art on diffusion models for visual computing. *arXiv preprint arXiv:2310.07204*, 2023.
- [48] Guocheng Qian, Jinjie Mai, Abdullah Hamdi, Jian Ren, Aliaksandr Siarohin, Bing Li, Hsin-Ying Lee, Ivan Skorokhodov, Peter Wonka, Sergey Tulyakov, et al. Magic123: One image to high-quality 3d object generation using both 2d and 3d diffusion priors. *Proc. ICLR*, 2024.
- [49] Colin Raffel, Noam Shazeer, Adam Roberts, Katherine Lee, Sharan Narang, Michael Matena, Yanqi Zhou, Wei Li, and Peter J Liu. Exploring the limits of transfer learning with a unified text-to-text transformer. *Proc. JMLR*, 2020.
- [50] Jiawei Ren, Liang Pan, Jiaxiang Tang, Chi Zhang, Ang Cao, Gang Zeng, and Ziwei Liu. DreamGaussian4D: Generative 4D Gaussian splatting. *arXiv preprint arXiv:2312.17142*, 2023.
- [51] Jiawei Ren, Kevin Xie, Ashkan Mirzaei, Hanxue Liang, Xiaohui Zeng, Karsten Kreis, Ziwei Liu, Antonio Torralba, Sanja Fidler, Seung Wook Kim, et al. L4gm: Large 4d gaussian reconstruction model. *arXiv preprint arXiv:2406.10324*, 2024.
- [52] Abhishek Sharma, Adams Yu, Ali Razavi, Andeep Toor, Andrew Pierson, Ankush Gupta, Austin Waters, Daniel Tanis, Dumitru Erhan, Eric Lau, Eleni Shaw, Gabe Barth-Maron, Greg Shaw, Han Zhang, Henna Nandwani, Hernan Moraldo, Hyunjik Kim, Irina Blok, Jakob Bauer, Jeff Donahue, Junyoung Chung, Kory Mathewson, Kurtis David, Lasse Espeholt, Marc van Zee, Matt McGill, Medhini Narasimhan, Miaosen Wang, Mikołaj Bińkowski, Mohammad Babaeizadeh, Mohammad Taghi Saffar, Nick Pezzotti, Pieter-Jan Kindermans, Poorva Rane, Rachel Hornung, Robert Riachi, Ruben Villegas, Rui Qian, Sander Dieleman, Serena Zhang, Serkan Cabi, Shixin Luo, Shlomi Fruchter, Signe Nørly, Srivatsan Srinivasan, Tobias Pfaff, Tom Hume, Vikas Verma, Weizhe Hua, William Zhu, Xinchen Yan, Xinyu Wang, Yelin Kim, Yuqing Du, and Yutian Chen. Veo, 2024.
- [53] Uriel Singer, Adam Polyak, Thomas Hayes, Xi Yin, Jie An, Songyang Zhang, Qiyuan Hu, Harry Yang, Oron Ashual, Oran Gafni, et al. Make-a-video: Text-to-video generation without text-video data. *Proc. ICLR*, 2023.
- [54] Uriel Singer, Shelly Sheynin, Adam Polyak, Oron Ashual, Iurii Makarov, Filippos Kokkinos, Naman Goyal, Andrea Vedaldi, Devi Parikh, Justin Johnson, et al. Text-to-4d dynamic scene generation. In *Proc. ICML*, 2023.
- [55] Qi Sun, Zhiyang Guo, Ziyu Wan, Jing Nathan Yan, Shengming Yin, Wengang Zhou, Jing Liao, and Houqiang Li. Eg4d: Explicit generation of 4d object without score distillation. *arXiv preprint arXiv:2405.18132*, 2024.

- [56] Hung-Yu Tseng, Qinbo Li, Changil Kim, Suhub Alsisan, Jia-Bin Huang, and Johannes Kopf. Consistent view synthesis with pose-guided diffusion models. In *Proc. CVPR*, 2023.
- [57] Thomas Unterthiner, Sjoerd van Steenkiste, Karol Kurach, Raphael Marinier, Marcin Michalski, and Sylvain Gelly. Towards accurate generative models of video: A new metric & challenges. *arXiv preprint arXiv:1812.01717*, 2018.
- [58] Lukas Uzolas, Elmar Eisemann, and Petr Kellnhofer. Motiondreamer: Zero-shot 3d mesh animation from video diffusion models. *arXiv preprint arXiv:2405.20155*, 2024.
- [59] Basile Van Hoorick, Rundi Wu, Ege Ozguroglu, Kyle Sargent, Ruoshi Liu, Pavel Tokmakov, Achal Dave, Changxi Zheng, and Carl Vondrick. Generative camera dolly: Extreme monocular dynamic novel view synthesis. *arXiv preprint arXiv:2405.14868*, 2024.
- [60] Ashish Vaswani, Noam Shazeer, Niki Parmar, Jakob Uszkoreit, Llion Jones, Aidan N Gomez, Łukasz Kaiser, and Illia Polosukhin. Attention is all you need. *Proc. NeurIPS*, 2017.
- [61] Vikram Voleti, Chun-Han Yao, Mark Boss, Adam Letts, David Pankratz, Dmitry Tochilkin, Christian Laforte, Robin Rombach, and Varun Jampani. Sv3d: Novel multi-view synthesis and 3d generation from a single image using latent video diffusion. *arXiv preprint arXiv:2403.12008*, 2024.
- [62] Wenjing Wang, Huan Yang, Zixi Tuo, Huiguo He, Junchen Zhu, Jianlong Fu, and Jiaying Liu. Videofactory: Swap attention in spatiotemporal diffusions for text-to-video generation. *arXiv preprint arXiv:2305.10874*, 2023.
- [63] Xiang Wang, Hangjie Yuan, Shiwei Zhang, Dayou Chen, Jiuniu Wang, Yingya Zhang, Yujun Shen, Deli Zhao, and Jingren Zhou. Videocomposer: Compositional video synthesis with motion controllability. *arXiv preprint arXiv:2306.02018*, 2023.
- [64] Yikai Wang, Xinzhou Wang, Zilong Chen, Zhengyi Wang, Fuchun Sun, and Jun Zhu. Vidu4d: Single generated video to high-fidelity 4d reconstruction with dynamic gaussian surfels. *arXiv preprint arXiv:2405.16822*, 2024.
- [65] Zhouxia Wang, Ziyang Yuan, Xintao Wang, Tianshui Chen, Menghan Xia, Ping Luo, and Yin Shan. Motionctrl: A unified and flexible motion controller for video generation. In *arXiv preprint arXiv:2312.03641*, 2023.
- [66] Daniel Watson, William Chan, Ricardo Martin-Brualla, Jonathan Ho, Andrea Tagliasacchi, and Mohammad Norouzi. Novel view synthesis with diffusion models. *Proc. ICLR*, 2023.
- [67] Daniel Watson, Saurabh Saxena, Lala Li, Andrea Tagliasacchi, and David J Fleet. Controlling space and time with diffusion models. *arXiv preprint arXiv:2407.07860*, 2024.
- [68] Chenfei Wu, Lun Huang, Qianxi Zhang, Binyang Li, Lei Ji, Fan Yang, Guillermo Sapiro, and Nan Duan. Godiva: Generating open-domain videos from natural descriptions. *arXiv preprint arXiv:2104.14806*, 2021.
- [69] Ruiqi Wu, , Liangyu Chen, Tong Yang, Chunle Guo, Chongyi Li, and Xiangyu Zhang. Lamp: Learn a motion pattern for few-shot-based video generation. *arXiv preprint arXiv:2310.10769*, 2023.
- [70] Zijie Wu, Chaohui Yu, Yanqin Jiang, Chenjie Cao, Fan Wang, and Xiang Bai. Sc4d: Sparse-controlled video-to-4d generation and motion transfer. *arXiv preprint arXiv:2404.03736*, 2024.
- [71] Zeqi Xiao, Yifan Zhou, Shuai Yang, and Xingang Pan. Video diffusion models are training-free motion interpreter and controller. *arXiv preprint arXiv:2405.14864*, 2024.
- [72] DeJia Xu, Hanwen Liang, Neel P Bhatt, Hezhen Hu, Hanxue Liang, Konstantinos N Plataniotis, and Zhangyang Wang. Comp4d: Llm-guided compositional 4d scene generation. *arXiv preprint arXiv:2403.16993*, 2024.
- [73] DeJia Xu, Weili Nie, Chao Liu, Sifei Liu, Jan Kautz, Zhangyang Wang, and Arash Vahdat. Camco: Camera-controllable 3d-consistent image-to-video generation. *arXiv preprint arXiv:2406.02509*, 2024.



- [74] Jun Xu, Tao Mei, Ting Yao, and Yong Rui. Msr-vtt: A large video description dataset for bridging video and language. In *Proc. CVPR*, 2016.
- [75] Zhongcong Xu, Jianfeng Zhang, Jun Hao Liew, Wenqing Zhang, Song Bai, Jiashi Feng, and Mike Zheng Shou. Pv3d: A 3d generative model for portrait video generation. *Proc. ICLR*, 2023.
- [76] Hongwei Xue, Tiankai Hang, Yanhong Zeng, Yuchong Sun, Bei Liu, Huan Yang, Jianlong Fu, and Baining Guo. Advancing high-resolution video-language representation with large-scale video transcriptions. In *Proc. CVPR*, 2022.
- [77] Qitong Yang, Mingtao Feng, Zijie Wu, Shijie Sun, Weisheng Dong, Yaonan Wang, and Ajmal Mian. Beyond skeletons: Integrative latent mapping for coherent 4d sequence generation. *arXiv preprint arXiv:2403.13238*, 2024.
- [78] Shiyuan Yang, Liang Hou, Haibin Huang, Chongyang Ma, Pengfei Wan, Di Zhang, Xiaodong Chen, and Jing Liao. Direct-a-video: Customized video generation with user-directed camera movement and object motion. *arXiv preprint arXiv:2402.03162*, 2024.
- [79] Zeyu Yang, Zijie Pan, Chun Gu, and Li Zhang. Diffusion<sup>2</sup>: Dynamic 3d content generation via score composition of orthogonal diffusion models. *arXiv preprint 2404.02148*, 2024.
- [80] Hu Ye, Jun Zhang, Sibio Liu, Xiao Han, and Wei Yang. Ip-adapter: Text compatible image prompt adapter for text-to-image diffusion models. *arXiv preprint arXiv:2308.06721*, 2023.
- [81] Yuyang Yin, DeJia Xu, Zhangyang Wang, Yao Zhao, and Yunchao Wei. 4dgen: Grounded 4d content generation with spatial-temporal consistency. *arXiv preprint arXiv:2312.17225*, 2023.
- [82] Yang You, Jing Li, Sashank Reddi, Jonathan Hseu, Sanjiv Kumar, Srinadh Bhojanapalli, Xiaodan Song, James Demmel, Kurt Keutzer, and Cho-Jui Hsieh. Large batch optimization for deep learning: Training bert in 76 minutes. *arXiv preprint arXiv:1904.00962*, 2019.
- [83] Heng Yu, Chaoyang Wang, Peiye Zhuang, Willi Menapace, Aliaksandr Siarohin, Junli Cao, Laszlo A Jeni, Sergey Tulyakov, and Hsin-Ying Lee. 4real: Towards photorealistic 4d scene generation via video diffusion models. *arXiv preprint arXiv:2406.07472*, 2024.
- [84] Jason J Yu, Fereshteh Forghani, Konstantinos G Derpanis, and Marcus A Brubaker. Long-term photometric consistent novel view synthesis with diffusion models. In *Proc. ICCV*, 2023.
- [85] Raza Yunus, Jan Eric Lenssen, Michael Niemeyer, Yiyi Liao, Christian Rupprecht, Christian Theobalt, Gerard Pons-Moll, Jia-Bin Huang, Vladislav Golyanik, and Eddy Ilg. Recent trends in 3d reconstruction of general non-rigid scenes. In *Computer Graphics Forum*, 2024.
- [86] Yifei Zeng, Yanqin Jiang, Siyu Zhu, Yuanxun Lu, Youtian Lin, Hao Zhu, Weiming Hu, Xun Cao, and Yao Yao. Stag4d: Spatial-temporal anchored generative 4d gaussians. *arXiv preprint arXiv:2403.14939*, 2024.
- [87] Haiyu Zhang, Xinyuan Chen, Yaohui Wang, Xihui Liu, Yunhong Wang, and Yu Qiao. 4diffusion: Multi-view video diffusion model for 4d generation. *arXiv preprint arXiv:2405.20674*, 2024.
- [88] Hao Zhang, Di Chang, Fang Li, Mohammad Soleymani, and Narendra Ahuja. Magic-pose4d: Crafting articulated models with appearance and motion control. *arXiv preprint arXiv:2405.14017*, 2024.
- [89] Lvmin Zhang, Anyi Rao, and Maneesh Agrawala. Adding conditional control to text-to-image diffusion models. *Proc. ICCV*, 2023.
- [90] Tianyuan Zhang, Hong-Xing Yu, Rundi Wu, Brandon Y Feng, Changxi Zheng, Noah Snavely, Jiajun Wu, and William T Freeman. Physdreamer: Physics-based interaction with 3d objects via video generation. *arXiv preprint arXiv:2404.13026*, 2024.
- [91] Wang Zhao, Shaohui Liu, Hengkai Guo, Wenping Wang, and Yong-Jin Liu. Particlesfm: Exploiting dense point trajectories for localizing moving cameras in the wild. In *Proc. ECCV*, 2022.

- [92] Yuyang Zhao, Zhiwen Yan, Enze Xie, Lanqing Hong, Zhenguo Li, and Gim Hee Lee. Animate124: Animating one image to 4d dynamic scene. *arXiv preprint arXiv:2311.14603*, 2023.
- [93] Yufeng Zheng, Xueting Li, Koki Nagano, Sifei Liu, Otmar Hilliges, and Shalini De Mello. A unified approach for text-and image-guided 4d scene generation. In *Proc. CVPR*, 2024.
- [94] Daquan Zhou, Weimin Wang, Hanshu Yan, Weiwei Lv, Yizhe Zhu, and Jiashi Feng. Magicvideo: Efficient video generation with latent diffusion models. *arXiv preprint arXiv:2211.11018*, 2022.
- [95] Tinghui Zhou, Richard Tucker, John Flynn, Graham Fyffe, and Noah Snavely. Stereo magnification: Learning view synthesis using multiplane images. *Proc. ACM TOG*, 2018.

Table 3: **Multi-view generation.** We evaluate all models using reference camera trajectories and single-view input images of the RealEstate10K test set. We compute reconstruction metrics based on the subsequent frames for the low-resolution and upsampled high-resolution generations.

Method	Low-resolution			High-resolution		
	PSNR ( $\uparrow$ )	SSIM ( $\uparrow$ )	LPIPS ( $\downarrow$ )	PSNR ( $\uparrow$ )	SSIM ( $\uparrow$ )	LPIPS ( $\downarrow$ )
Base Model	14.74	0.320	0.334	13.23	0.459	0.572
MotionCtrl	15.07	0.348	0.308	13.42	0.467	0.560
MotionCtrl (frozen)	14.59	0.308	0.340	13.11	0.455	0.573
CameraCtrl	14.81	0.327	0.330	13.21	0.456	0.571
Ours	<b>17.23</b>	<b>0.534</b>	<b>0.211</b>	<b>14.90</b>	<b>0.499</b>	<b>0.499</b>
w/o Plucker	14.89	0.346	0.308	13.05	0.455	0.573
w/o ControlNet	14.66	0.313	0.340	13.10	0.450	0.573
w/o weight copy	16.96	0.509	0.220	14.75	0.495	0.504

Table 4: **Quality metrics evaluation.** We evaluate all models using text prompts from the RealEstate10K and MSR-VTT test sets respectively.

Method	RealEstate10K			MSR-VTT		
	FID ( $\downarrow$ )	FVD ( $\downarrow$ )	CLIPSIM ( $\uparrow$ )	FID ( $\downarrow$ )	FVD ( $\downarrow$ )	CLIPSIM ( $\uparrow$ )
Base Model	8.22	160.37	0.2677	<b>3.50</b>	<b>141.26</b>	<b>0.2774</b>
MotionCtrl	1.50	52.30	0.2708	9.97	183.57	0.2677
MotionCtrl (frozen)	3.53	142.15	0.2772	8.19	165.48	0.2679
CameraCtrl	2.28	66.31	0.2730	8.47	181.90	0.2690
Ours	1.40	42.43	<b>0.2807</b>	7.80	165.18	0.2689
w/o Plucker	<b>1.17</b>	43.65	0.2715	9.84	152.91	0.2660
w/o ControlNet	3.66	137.06	0.2766	8.34	185.79	0.2674
w/o weight copy	1.38	<b>42.00</b>	0.2710	10.09	218.43	0.2647

## A Quantitative evaluation

We further evaluate all models for the task of single image-to-multiview generation. Furthermore, we provide results for established 2D video generation metrics.

### A.1 Multi-view generation

We evaluate our model for image-to-multiview generation. Due to ground truth correspondences for the RealEstate10K [95] dataset, we can condition our model on a given camera trajectory and assess image based metrics, i.e., PSNR, SSIM, and LPIPS. We provide results for the low-resolution base model and the upsampled high-resolution results in Tab. 3.

### A.2 Quality metrics

Moreover, we evaluate all models on established image and video generation metrics, namely, FID [21], FVD [57], and CLIPSIM [68]. We provide results for RealEstate10K [95] and MSR-VTT [74] in Tab. 4.